Acta Crystallographica Section F
Structural Biology and Crystallization Communications
ISSN 1744-3091

Jantana Wongsantichon,[a] Jirundon Yuvaniyama[b] and Albert J. Ketterman[a]*

[a]Institute of Molecular Biology and Genetics, Mahidol University, Salaya Campus, Nakorn Pathom 73170, Thailand, and [b]Department of Biochemistry and Center for Excellence in Protein Structure and Function, Faculty of Science, Mahidol University, Rama 6 Road, Phayathai, Bangkok 10400, Thailand

Correspondence e-mail: frakt@mahidol.ac.th

Received 26 October 2005
Accepted 22 February 2006

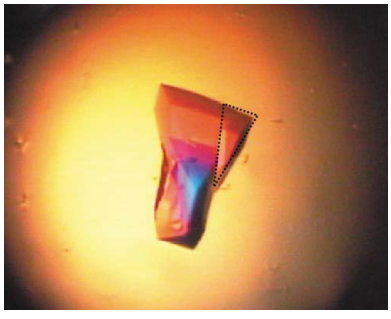

© 2006 International Union of Crystallography
All rights reserved

Crystallization and preliminary X-ray crystallographic analysis of a highly stable mutant V107A of glutathione transferase from *Anopheles dirus* in complex with glutathione

An engineered mutant V107A of the dimeric glutathione transferase enzyme from *Anopheles dirus* (adgstD4-4) was cocrystallized with glutathione substrate using the hanging-drop vapour-diffusion method. The crystal diffracted to 2.47 Å resolution in space group $P3_221$ (unit-cell parameters $a = b = 49.4$, $c = 272.4$ Å). Although the crystal morphology differed from that previously obtained for the wild-type enzyme, the crystal packing was the same. At 318 K, the engineered mutant showed an enzyme stability that was increased by about 32-fold, while possessing a similar catalytic function to the wild type. Structural determination will provide valuable understanding of the role of Val107. This residue is in the dimeric interface and appears to contribute towards enhancing the physical properties of the entire protein.

1. Introduction

Glutathione transferases (GSTs; EC 2.5.1.18) are dimeric enzymes involved in phase II detoxication processes by conjugation of a thiol group from reduced glutathione (γ-glutamyl-cysteinyl-glyine; GSH) to an electrophilic centre of diverse xenobiotic compounds, producing less reactive and more polar substances in order to facilitate elimination from cells (Armstrong, 1991; Mannervik & Danielson, 1988). Cytosolic GSTs are generally found as multiple isoenzymes within organisms and with varying substrate selectivity (Hayes *et al.*, 2005; Hayes & Pulford, 1995). In the various GST dimeric structures, subunits are assembled by twofold symmetry, with subunit interactions that vary between the GST classes but generate a buried interface area of about 2700–3400 Å^2 (Dixon *et al.*, 2002). Therefore, homodimeric or heterodimeric GSTs are only formed by subunits from the same gene class and with comparable molecular recognition at the subunit interface.

The structural model of the wild-type GST adgstD4-4 from *Anopheles dirus* shows that Val107 is located in the subunit-interface region of the dimeric GST, forming part of an intersubunit lock-and-key 'clasp' motif (Oakley, Harnnoi *et al.*, 2001; Wongsantichon & Ketterman, 2006). The 'key' residue not only inserts into a hydrophobic pocket of the neighbouring subunit, but also itself acts as part of the 'lock' for the other subunit 'key'. In addition, the 'key' residues from both subunits hook around each other in an aromatic π–π interaction through slightly offset aromatic ring stacking, generating a 'clasp' in the middle of the subunit interface. A special characteristic of the motif is to stabilize the GST dimeric structure in the middle region of the twofold axis. The motif was found to be highly conserved in many classes of insect GSTs, as shown by primary sequence alignments (Wongsantichon & Ketterman, 2006). The available crystal structures of insect-specific δ-class GSTs such as *Lucilia* GST (Wilce *et al.*, 1994, 1995), adgstD3-3 (PDB code 1jlv; Oakley, Harnnoi *et al.*, 2001), adgstD4-4 (PDB code 1jlw; Oakley, Harnnoi *et al.*, 2001), adgstD5-5 (PDB code 1r5a; Udomsinprasert *et al.*, 2005), adgstD6-6 (PDB code 1v2a; Udomsinprasert *et al.*, 2005) and aggstD1-6 (PDB code 1pn9; Chen *et al.*, 2003) also reveal the highly conserved clasp-like motif (Wongsantichon & Ketterman, 2006). In the apo structure of adgstD4-4, the residue Val107 is also part of the wall of the active site. This residue's surface area is about 100–130 Å^2 and is only exposed to solvent in the active-site pocket. However, the residue is also part of the first-sphere interaction of

Leu103, which generates a small hydrophobic core interior to the active site and subunit interface (Wongsantichon *et al.*, 2003). In addition to this spatial motif, adgstD4-4 also possesses several other intersubunit interactions which contribute to interface formation, as previously discussed in Wongsantichon & Ketterman (2005). The Val107 residue has been studied by substitution with six different amino acids of various sizes and properties in order to elucidate its role in the dimeric enzyme (Wongsantichon & Ketterman, 2006). All engineered mutants were found to be catalytically active, demonstrating the presence of dimeric active forms, which suggests that the residue position is not critical for dimerization. Steady-state kinetics studies using GSH and CDNB as co-substrates show that substitutions by hydrophobic and uncharged residues at the Val107 position have no effect on the catalytic properties, whereas positively and negatively charged residues diminish the enzyme catalytic rate (k_{cat}) and weaken the binding affinity towards GSH substrate (K_m), with positive cooperativity observed upon binding. In this regard, charged residue replacements were considered to be unfavourable in the region. However, all engineered mutants appeared to enhance thermal stability as demonstrated by a heat-inactivation assay at 318 K, suggesting that the residue also plays a role in structural stabilization. Of the mutants, adgstD4-4 V107A shows the greatest half-life (390.2 $\pm$ 22.4 min), which is about 32 times that of the wild type (12.3 $\pm$ 0.9 min). There is no marked alteration in the secondary or tertiary structure of V107A as shown by far-UV circular dichroism and tryptophan intrinsic fluorescence, respectively. Nevertheless, conformational rearrangement at the quaternary structural level or subunit dimerization of the engineered enzyme was observed by fluorescence dye binding using 1-anilinonaphthalene-8-sulfonic acid (ANS), which is reported to bind in the hydrophobic cleft along the dimeric interface in GST class α (Sayed *et al.*, 2002). As shown by the above data, substitution of valine by alanine at position 107 in adgstD4-4 appears to be structurally important and alters the enzyme stability and subunit dimerization, while maintaining similar catalytic properties to the wild type. Therefore, structural determination of the mutant is of interest and would be useful in understanding the protein structure–function correlation, particularly for enzyme stability.

2. Material and methods

2.1. Construction and purification of V107A

A single point mutation of *A. dirus* glutathione transferase isoform 4 (adgstD4-4) was obtained by PCR-based site-directed mutagenesis, replacing valine with alanine at position 107 using the Stratagene Quick Change site-directed mutagenesis kit (Stratagene). The engineered enzyme was overexpressed by 0.1 m*M* IPTG (isopropyl 1-thio-β-D-galactopyranoside) induction at 298 K in *Escherichia coli* BL21(DE3) pLysS as soluble protein and was purified using GSTrap FF affinity chromatography (Amersham Pharmacia) as previously described (Wongtrakul *et al.*, 2003).

2.2. Crystallization and X-ray data collection

The purified protein was concentrated using an Amicon Ultra-15 centrifugal filter device (Millipore) with 10 kDa cutoff and filtered through an Ultrafree-MC 0.22 µm centrifugal filter unit (Millipore). Prior to crystallization, the protein concentration was adjusted to 9 mg ml^{-1} in 50 m*M* Tris–HCl pH 7.5, 10 m*M* DTT in the presence of 10 m*M* GSH substrate. The hanging-drop vapour-diffusion method was used with a crystallization droplet comprising of 2 µl protein solution and 2 µl reservoir solution consisting of 0.1 *M* imidazole pH 7.0, 0.35 *M* ammonium acetate and 30%(*w*/*v*) polyethylene glycol (PEG) 4000. The volume of solution in the reservoir was 0.5 ml. Crystals appeared within one week at 295 K. A single prismatic crystal with dimensions 0.46 $\times$ 0.30 $\times$ 0.18 mm was obtained; it was dissected into a smaller piece of dimensions 0.28 $\times$ 0.08 $\times$ 0.07 mm and briefly soaked in a cryosolution consisting of 0.1 *M* imidazole pH 7.0, 0.368 *M* ammonium acetate, 32%(*w*/*v*) PEG 4000 and 10%(*v*/*v*) glycerol before being flash-frozen in a liquid-nitrogen stream at 110 K.

X-ray diffraction data were collected at the Center for Excellence in Protein Structure and Function, Faculty of Science, Mahidol University, Thailand. X-ray diffraction patterns were recorded on an R-AXIS IV^{++} image-plate system (Rigaku/MSC) using Cu $K\alpha$ radiation from a Rigaku RU-H3R rotating-anode X-ray generator operating at 50 kV and 100 mA equipped with Osmic Confocal Maxflux multi-layer optics and a 0.3 mm collimator. The crystal was flash-frozen using an X-Stream 2000 low-temperature system (Rigaku/MSC). Data were processed and scaled using the *CrystalClear*/*d***TREK* program suite (Pflugrath, 1999).

3. Results and discussion

After initial screening, the crystallization conditions were optimized by varying the pH of the buffer from 4.6 to 7.5 and the concentration of ammonium acetate from 0.25 to 0.40 *M*. Two different crystal morphologies, fine rod-shaped and prism-shaped, were obtained from the screening in 0.1 *M* imidazole pH 7.0 within a week. A single prism-shaped crystal chosen for X-ray diffraction was obtained from conditions consisting of 32%(*w*/*v*) PEG 4000, 0.35 *M* ammonium acetate, 0.1 *M* imidazole pH 7.0 in the presence of 10 m*M* GSH. However, owing to its large dimensions of 0.46 $\times$ 0.30 $\times$ 0.18 mm, as shown in Fig. 1, a glass fibre was used to dissect the crystal to a smaller volume to facilitate freezing on a cryoloop. The crystal slice was briefly soaked in a cryosolution consisting of reservoir solution containing 10%(*v*/*v*) glycerol and approximately 5% higher concentrations of PEG 4000 and ammonium acetate. The crystal slice was flash-frozen in a liquid-nitrogen stream. Diffraction data were collected to an effective resolution of 2.47 Å using a 240 mm crystal-to-detector distance with an exposure time of 150 s and covering 0.25° oscillation per image (Fig. 2).

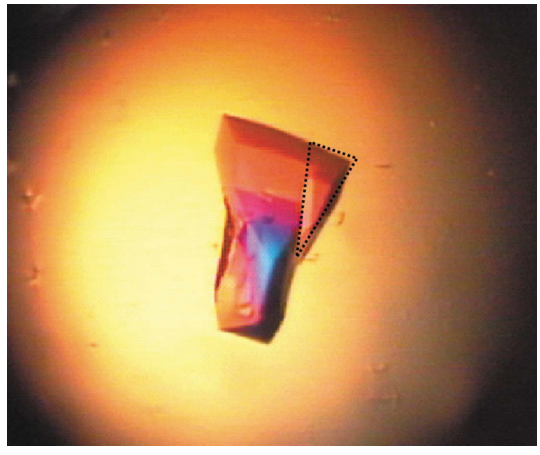

Figure 1
A prism-shaped crystal of adgstD4-V107A photographed under polarized light. The crystal size is 0.46 $\times$ 0.30 $\times$ 0.18 mm for the largest dimensions. The dotted triangle represents the crystal slice that was used for X-ray diffraction.

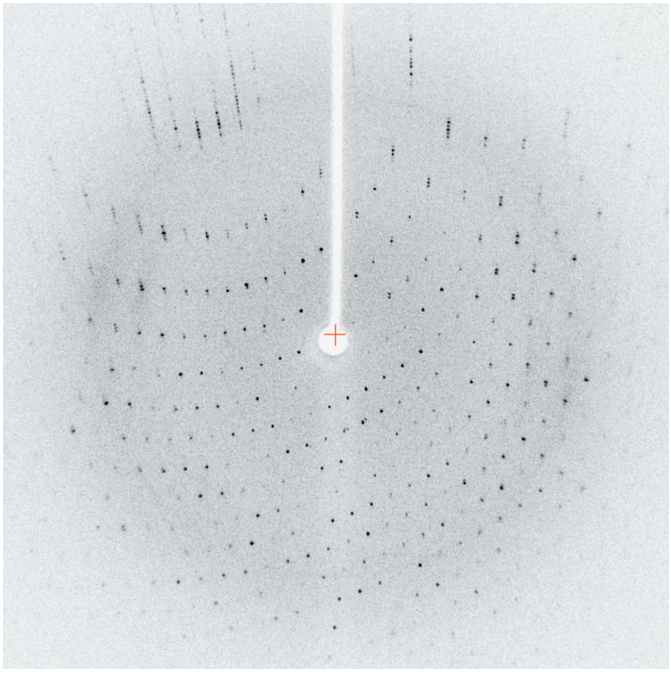

Figure 2
A 0.25° rotation photograph showing the X-ray diffraction pattern from the crystal slice.

The engineered mutant in this study can also be crystallized using the conditions previously reported for the wild-type enzyme (Oakley, Jirajaroenrat *et al.*, 2001), consisting of 30%(*w*/*v*) PEG 8000, 0.2 *M* sodium acetate and 0.1 *M* sodium cacodylate pH 6.5, generating fine rod-shaped crystals. In this regard, the present study demonstrates that different crystal morphologies can be derived from different crystallization conditions. However, preliminary X-ray crystallographic analysis shows that the diffraction patterns of a prism-shaped crystal from the engineered mutant and of a rod-shaped $P3_221$ crystal of the wild type (PDB code 1jlw) are isomorphous (Oakley, Jirajaroenrat *et al.*, 2001). Diffraction spots of the mutant were initially scaled and merged in space group *P*321 (as summarized in Table 1) even though they showed absences that could be characteristic of either of the trigonal space groups $P3_121$ or $P3_221$. This was to preserve all the data for subsequent verification of the correct space group by molecular-replacement calculations. The initial phases of the adgstD4-4 V107A structure were determined with *AMoRe* from the *CCP*4 program suite (Collaborative Computational Project, Number 4, 1994; Navaza, 1994) using chain *A* of the wild-type structure as a search model. Translation searches in the three space groups *P*321, $P3_121$ and $P3_221$ showed a good result for calculation in space group $P3_221$, which gave an amplitude correlation coefficient (CC) of 43.1% and an *R* factor of 48.1% for the best solution, compared with CC = 20.7%, *R* = 56.6% and CC = 23.1%, *R* = 55.0% for the other two space groups. Addition of the second molecule resulted in a CC of 72.3% on amplitude and 76.4% on intensity with an *R* factor of 35.8% after the fitting calculation. Examination of the best solution revealed good crystal packing and no clashes between symmetry-related molecules. This shows that the molecular packing is preserved, suggesting that the V107A mutation and the presence of GSH do not cause large structural deviation from the non-ligand-bound wild-type structure. This preliminary model of the engineered mutant is currently being refined and will be further studied to investigate the marked increase in structural stability.

Table 1
Data-collection statistics for adgstD4-4 V107A crystals in complex with GSH.

Values in parentheses correspond to the highest resolution shell.

Space group	$P3_221$
Unit-cell parameters	
a, *b* (Å)	49.4
c (Å)	272.4
α, β (°)	90
γ (°)	120
Unit-cell volume (Å^3)	575799
Resolution limits (Å)	42.78–2.47 (2.56–2.47)
No. of observed reflections	65482
No. of unique reflections	14436
Completeness (%)	95.3 (80.0)
Multiplicity	2.55 (1.5)
$R_{\rm merge}$† (%)	10.2 (16.8)
$\langle I/\sigma(I)\rangle$	4.9 (2.2)
$V_{\rm M}$ (Å^3 Da^{-1})	1.9
Solvent content (%)	35.4
No. of molecules per ASU	2

† $R_{\rm merge} = \sum_{hkl}\sum_i |I_i(hkl) - \langle I(hkl)\rangle| / \sum_{hkl}\sum_i I_i(hkl)$, where I_i is the intensity of the *i*th measurement of an equivalent reflection with indices *hkl*.

This work was supported by a grant from the Thailand Research Fund to AJK and a Royal Golden Jubilee scholarship to JW.

References

Armstrong, R. N. (1991). *Chem. Res. Toxicol.* **4**, 131–140.
Chen, L., Hall, P. R., Zhou, X. E., Ranson, H., Hemingway, J. & Meehan, E. J. (2003). *Acta Cryst.* D**59**, 2211–2217.
Collaborative Computational Project, Number 4 (1994). *Acta Cryst.* D**50**, 760–763.
Dixon, D. P., Lapthorn, A. & Edwards, R. (2002). *Genome Biol.* **3**, 1–10.
Hayes, J. D., Flanagan, J. U. & Jowsey, I. R. (2005). *Annu. Rev. Pharmacol. Toxicol.* **45**, 51–88.
Hayes, J. D. & Pulford, D. J. (1995). *CRC Crit. Rev. Biochem. Mol. Biol.* **30**, 445–600.
Mannervik, B. & Danielson, U. H. (1988). *CRC Crit. Rev. Biochem.* **23**, 283–337.
Navaza, J. (1994). *Acta Cryst.* A**50**, 157–163.
Oakley, A. J., Harnnoi, T., Udomsinprasert, R., Jirajaroenrat, K., Ketterman, A. J. & Wilce, M. C. J. (2001). *Protein Sci.* **10**, 2176–2185.
Oakley, A. J., Jirajaroenrat, K., Harnnoi, T., Ketterman, A. J. & Wilce, M. C. J. (2001). *Acta Cryst.* D**57**, 870–872.
Pflugrath, J. W. (1999). *Acta Cryst.* D**55**, 1718–1725.
Sayed, Y., Hornby, J. A. T., Lopez, M. & Dirr, H. (2002). *Biochem. J.* **363**, 341–346.
Udomsinprasert, R., Pongjaroenkit, S., Wongsantichon, J., Oakley, A. J., Prapanthadara, L., Wilce, M. C. J. & Ketterman, A. J. (2005). *Biochem. J.* **388**, 763–771.
Wilce, M. C. J., Board, P. G., Feil, S. C. & Parker, M. W. (1995). *EMBO J.* **14**, 2133–2143.
Wilce, M. C. J., Feil, S. C., Board, P. G. & Parker, M. W. (1994). *J. Mol. Biol.* **236**, 1407–1409.
Wongsantichon, J., Harnnoi, T. & Ketterman, A. J. (2003). *Biochem. J.* **373**, 759–765.
Wongsantichon, J. & Ketterman, A. (2005). *Methods Enzymol.* **401**, 100–116.
Wongsantichon, J. & Ketterman, A. J. (2006). *Biochem. J.* **394**, 135–144.
Wongtrakul, J., Udomsinprasert, R. & Ketterman, A. (2003). *Insect Biochem. Mol. Biol.* **33**, 971–979.